Volume 10 | Number 33 | 7 September 2019 | Pages 7661–7824

Chemical Science

rsc.li/chemical-science

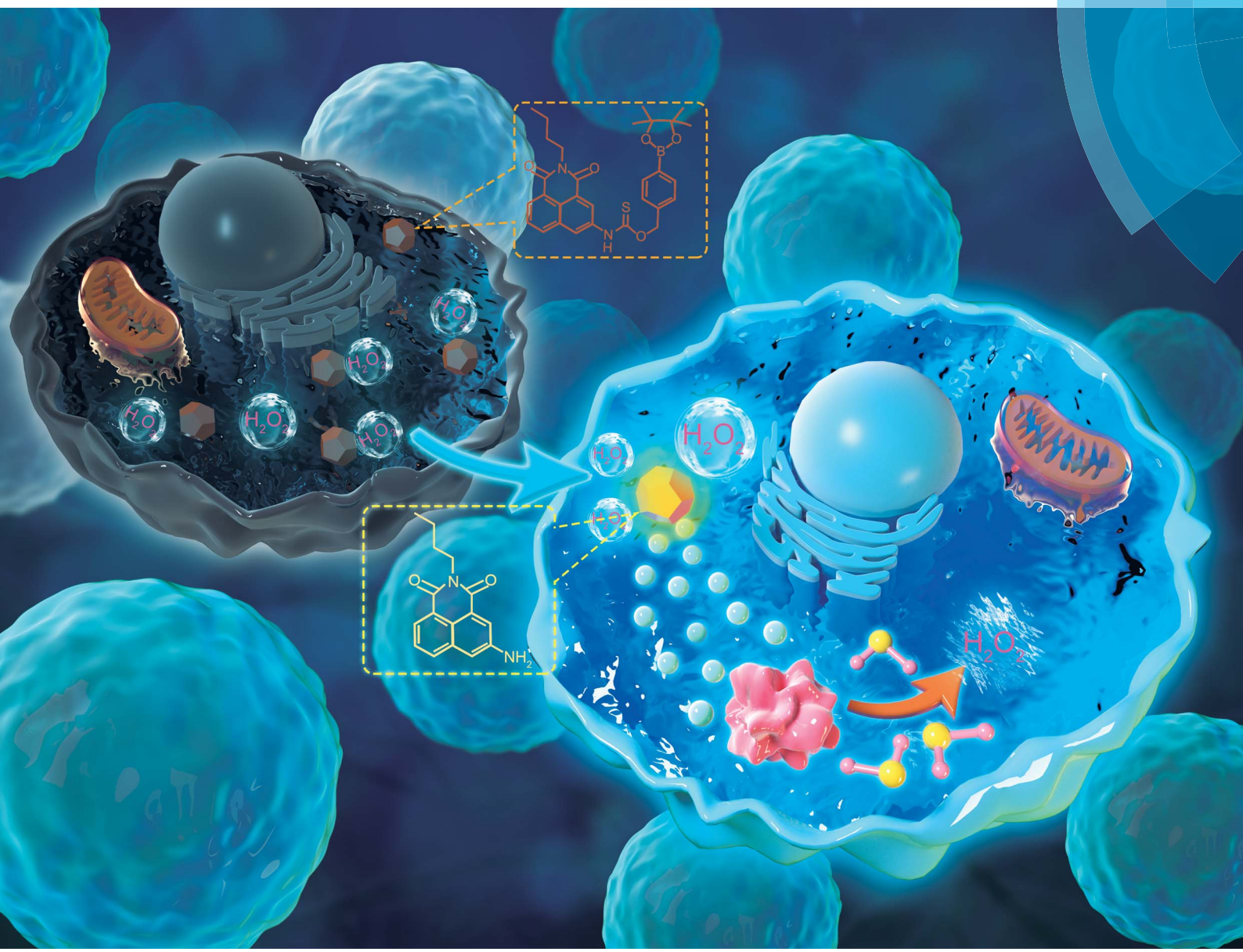

ISSN 2041-6539

ROYAL SOCIETY OF CHEMISTRY | Celebrating IYPT 2019

EDGE ARTICLE

Huimin Ma *et al.*

Reactive oxygen species-triggered off-on fluorescence donor for imaging hydrogen sulfide delivery in living cells

Chemical Science

EDGE ARTICLE

View Article Online
View Journal | View Issue

Cite this: *Chem. Sci.*, 2019, **10**, 7690

All publication charges for this article have been paid for by the Royal Society of Chemistry

Reactive oxygen species-triggered off-on fluorescence donor for imaging hydrogen sulfide delivery in living cells†

Yiming Hu,[ab] Xiaoyi Li,[a] Yu Fang,[a] Wen Shi,[ab] Xiaohua Li,[a] Wei Chen,[c] Ming Xian[c] and Huimin Ma*[ab]

Received 13th May 2019
Accepted 8th July 2019

DOI: 10.1039/c9sc02323b

rsc.li/chemical-science

Hydrogen sulfide (H_2S), an important gasotransmitter, can mediate a variety of pathophysiological processes, and H_2S-based donors have been intensively explored for the therapy of cardiovascular injury, nerve damage and intestinal disorders. However, most of the H_2S donors are not capable of simultaneously real-time tracking intracellular H_2S delivery, which limits their biological application for elucidating the specific function of H_2S. Herein we develop the first reactive oxygen species (ROS)-triggered off-on fluorescence H_2S donor (NAB) by incorporating ROS-responsive arylboronate into a fluorophore through thiocarbamate. The donor NAB can release carbonyl sulfide (COS) and the fluorophore with a fluorescence off-on response *via* a ROS-triggered self-immolative reaction, and then COS is quickly converted to H_2S by the ubiquitous carbonic anhydrase. This dual function makes NAB suitable for not only *in situ* and real-time monitoring of the intracellular H_2S release but also rescuing RAW264.7 cells from the hazardous oxidative environment under the stimulation of phorbol-12-myristate-13-acetate, revealing the possible potential of NAB as a therapeutic prodrug with the fluorescence imaging capacity.

Introduction

Hydrogen Sulfide (H_2S) is an important gasotransmitter, which can mediate a variety of physiological and pathological processes. Recent studies have demonstrated that H_2S is associated with iron homeostasis,[1] vasodilation[2] and neurotransmission.[3] Modulation of H_2S levels is suggested to have potential therapeutic value. However, further understanding the biological function of H_2S remains an open challenge due to the lack of effective tools to modulate and monitor cellular H_2S levels. Some inorganic sulfide salts (NaSH, Na_2S, *etc*) and commercially available GYY4137 can be used for H_2S delivery, but they suffer from uncontrollable releasing efficiency and imaging inability, which limits their application in cells. So far, some synthetic donors have been reported,[4] which can be activated by controllable manners, such as pH modulation,[5] cellular amines,[6] thiols,[7] enzymes,[8] light,[9] bio-orthogonal reaction,[10] and reactive oxygen species (ROS).[11] Despite the great progresses in researching the biological roles of H_2S, these donors always need additional analytical methods to verify H_2S release. Fluorescence spectroscopy has attracted much attention because of its great temporal and spatial sampling capability as well as high sensitivity.[12] We envision that it should be highly favorable for *in situ* and real-time monitoring of H_2S release in complex biological systems if a controllable H_2S donor can release H_2S accompanied by fluorescence change. However, such H_2S donors are still rare.

Herein, we design the first ROS-triggered fluorescence H_2S donor (NAB; Fig. 1A), which is constructed by linking ROS-responsive arylboronate to the fluorophore of 3-amino-*N*-butyl-1,8-naphthalimide (NAH) with thiocarbamate (Scheme S1; Fig. S1–S6†). NAB itself emits rather weak fluorescence; upon reaction with ROS, the donor NAB releases carbonyl sulfide (COS) and the strongly fluorescent NAH *via* a self-immolative reaction. Then COS is quickly transformed to H_2S by the ubiquitous enzyme of carbonic anhydrase (CA). As a result, H_2S delivery is achieved by NAB, concomitant with an off-on fluorescence, which can be used for *in situ* and real time monitoring of H_2S release in living biosystems such as cells.

Results and discussion

Spectroscopic response of NAB to ROS

The reaction of NAB with H_2O_2 was investigated in the phosphate buffer (20 mM, pH 7.4). NAB displayed a maximum

[a]*Beijing National Laboratory for Molecular Sciences, Key Laboratory of Analytical Chemistry for Living Biosystems, Institute of Chemistry, Chinese Academy of Sciences, Beijing 100190, China. E-mail: mahm@iccas.ac.cn*

[b]*University of Chinese Academy of Sciences, Beijing 100049, China*

[c]*Department of Chemistry, Washington State University, Pullman, Washington 99164, USA*

† Electronic supplementary information (ESI) available. See DOI: 10.1039/c9sc02323b

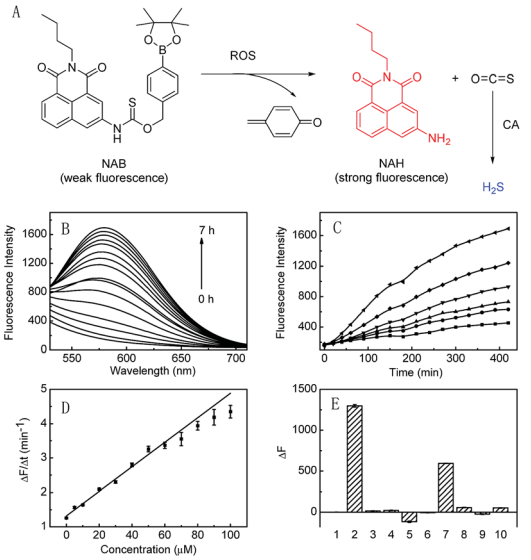

Fig. 1 (A) Response mechanism of H_2S donation from NAB with ROS. (B) Fluorescence spectra of NAB (10 μM) with H_2O_2 (100 μM) at varied time in phosphate buffer (20 mM, pH 7.4). (C) Fluorescence kinetic curves of NAB (10 μM) with varied H_2O_2 (from bottom to top): 0 (control), 5, 10, 20, 50, 100 μM. (D) Linear fitting curve of the initial rate of fluorescence intensity changes toward the concentration of H_2O_2 in the range of 0–100 μM. (E) Fluorescence changes of NAB (10 μM) in the presence of different ROS species: (1) NAB only; (2) H_2O_2 (100 μM); (3) NO (100 μM); (4) OCl^- (100 μM); (5) $^{\bullet}OH$ (100 μM); (6) $^1O_2$ (100 μM); (7) $O_2^{\bullet-}$ (100 μM); (8) TBHP (100 μM); (9) $TBO^{\bullet}$ (100 μM); (10) $ONOO^-$ (10 μM). $\lambda_{ex/em}$ = 405/577 nm.

absorption at 300 nm, and the corresponding fluorophore NAH displayed two absorption peaks at 346 nm and 405 nm (Fig. S7A†). However, addition of H_2O_2 to NAB caused a remarkable decrease of the absorption peak at 300 nm, accompanying the formation of a spectrum similar to that of NAH (Fig. S7A†). Moreover, NAB itself produced faint fluorescence signal under the excitation wavelength of 405 nm, and its reaction solution with H_2O_2 showed a fluorescence emission peak at 577 nm, which is in agreement with the fluorescence spectrum of NAH (Fig. S7B†). The reaction products of NAB with H_2O_2 were further analyzed by mass spectrum. As depicted in Fig. S8,† the ESI-MS spectrum of the reaction solution shows a mass peak at m/z = 267.2 ($[M–H]^-$), which is the same as that of NAH. The above results clearly indicate that the reaction of NAB with H_2O_2 yields the strongly fluorescent NAH.

It was noted that the conversion of NAB to NAH was incomplete even after 7 h according to the spectra of NAH (Fig. S7†). Furthermore, the time-dependent fluorescence responses of NAB to varied H_2O_2 also revealed that NAB could be used as a controllable H_2S donor by H_2O_2 (Fig. 1). The initial rate of fluorescence increase at varied concentrations of H_2O_2 displayed good linearity with an equation of $\Delta F/\Delta t = 0.0357 \times [H_2O_2]$ (μM) + 1.32 (R = 0.990) in the range of 0–100 μM H_2O_2 (Fig. 1D). The lowest triggering concentration of H_2O_2 that NAB needed was 2.21 μM (k = 3), which was higher than the reported physiological concentration (usually ≤0.7 μM) of intracellular H_2O_2,[13] implying that NAB was probably unable to deliver H_2S at the normal level of intracellular H_2O_2 with the exception of some situations over 2.21 μM H_2O_2 caused by other stimulations.

The effects of pH and temperature were also studied. As shown in Fig. S9,† the reaction between NAB and H_2O_2 remains inert under the acidic environment, but the fluorescence intensity is dramatically increased along with the rise in pH value. It might be due to the fact that alkaline media could accelerate the hydrolysis of the aryl-boronic esters to the corresponding phenols.[14] Although higher temperature was favorable for the reaction, NAB also worked effectively under the physiological conditions (37 °C, pH 7.4).

Then we tested the fluorescent response of NAB to various ROS. As depicted in Fig. 1E, NAB exhibits the strongest response to H_2O_2 over the other ROS, among which $O_2^{\bullet-}$ showed some response because it is the precusor of H_2O_2.[15] This indicates that ROS, in particular their representative H_2O_2 (the most abundant one in cells),[16] can effectively trigger the H_2S release of NAB. The selectivity of NAB was examined over other potential interfering species in living cells, such as inorganic salts (KCl, $MgCl_2$, $CaCl_2$, $ZnCl_2$), glucose, vitamin C, glutathione and amino acids (glycine, cysteine, lysine, glutamic acid and alanine). As shown in Fig. S10,† NAB displays high selectivity for H_2O_2 over the other tested species.

Methylene blue colorimetric method for H_2S detection

To verify if the decomposed product of NAB could be converted to H_2S in the presence of CA, the well-known methylene blue method[11] was used to measure the H_2S generation, by which the generation of H_2S can be proved by the formation of methylene blue that has a characteristic absorption peak at 670 nm. As shown in Fig. S11,† the mixture of the MB solution and the NAB solution with H_2O_2 indeed produces an apparent absorption peak at 670 nm, clearly indicating the H_2S release by NAB. However, when acetazolamide, a CA inhibitor, was added to the reaction system, the absorbance at 670 nm was significantly suppressed, revealing that the H_2S release of NAB was dependent on CA in the COS-to-H_2S conversion.

Based on the H_2S calibration curve (Fig. S11B†), 10, 20 and 30 μM of NAB could generate 2.3, 3.6 and 5.0 μM of H_2S, respectively, within 7 h, revealing a non-quantitative H_2S release of NAB. The reason for this phenomenon may be complicated, but H_2O_2 may be one of the influence factors. As shown in Fig. S12,† more H_2O_2 (>100 μM) can cause a significant decrease of absorbance at 670 nm. Thus, a further study on H_2O_2 effect was made. The influence of H_2O_2 on MB itself was excluded first (Fig. S13†). Then, 10 μM Na_2S solution was mixed with varied H_2O_2 (100–300 μM) for 0.5 h and the mixture was transferred to the MB solution for measurement. As depicted in Fig. S14,† the MB formation is inhibited significantly, and this inhibition is H_2O_2- and time-dependent. For instance, prolonging the reaction time between Na_2S and 300 μM H_2O_2 to 7 h resulted in the decrease of absorbance at 670 nm nearly to zero (Fig. S14†), which suggested that H_2O_2 may deplete H_2S in this case, probably *via* an oxidizing action. Conversely, such an action

means that the released H_2S from NAB may scavenge H_2O_2, thereby relieving the oxidative stress.

Cytotoxicity of NAB

The toxicity of NAB was evaluated with HeLa and RAW264.7 cells (these two kinds of cell lines were obtained from Nanjing KeyGEN BioTECH Co., LTD, China) by standard MTT assay. As shown in Fig. S15†,† cell viability of both cell lines is not significantly affected by the incubation with NAB for 24 h, suggesting the good biocompatibility of the donor.

Fluorescence imaging of H_2S release in living cells

As mentioned above, reaction of NAB with H_2O_2 can produce fluorescence off-on response, thus this behavior was investigated to image the H_2S release from the donor in living cells. As shown in Fig. S16,† the NAB-loaded HeLa cells scarcely exhibit fluorescence, but display a gradually increased fluorescence with time upon addition of H_2O_2. Moreover, the fluorescence became much brighter when the concentration of H_2O_2 was elevated from 50 μM to 100 μM (Fig. 2). Nevertheless, after pretreated with NAC (an antioxidant to scavenge H_2O_2), the cells exhibited significantly decreased fluorescence (Fig. 2B). These results demonstrate the triggering ability of ROS in the fluorescence signal of NAB in cells.

To verify the intracellular ROS-triggered H_2S release, a commercially available probe (WSP-1), whose fluorescence can be selectively turned on by H_2S,[17] was used for the detection of H_2S in HeLa cells. As shown in Fig. S17 (images c–e),† the fluorescence of WSP-1 in the green channel rises with increasing the dose of NAB in the presence of H_2O_2, suggesting the generation of the gradually increased H_2S. However, the fluorescence signal was largely attenuated when the cells were incubated with much more H_2O_2 (Fig. S18†), which is consistent with the aforementioned MB test results, that is, the released H_2S from NAB may be consumed by excess H_2O_2. These results validated NAB as the fluorescence donor for H_2S delivery, and suggested that our dual-functional donor could be used as a fluorescent probe for real time monitoring of the H_2S release in cells.

H_2S release by endogenous ROS in living cells

To evaluate the ability of NAB to release H_2S *via* endogenous ROS in living cells, RAW264.7 cells were chosen as a model because they are believed to generate a considerable amount of ROS in inflammatory pathology induced by PMA.[18] As shown in Fig. 3, RAW264.7 cells pretreated with PMA for 1 h and then with NAB for 4 h display a remarkable fluorescence increase when compared to the control group without PMA, and the fluorescence further increases with the treatment of more PMA. This indicates that NAB can release H_2S *via* the endogenous ROS. Similarly, such a fluorescence increase can be efficiently inhibited by NAC, which is consistent with the above results in HeLa cells. Taking together, NAB may be capable of releasing H_2S under pathological ROS levels and *in situ* imaging this event in cells.

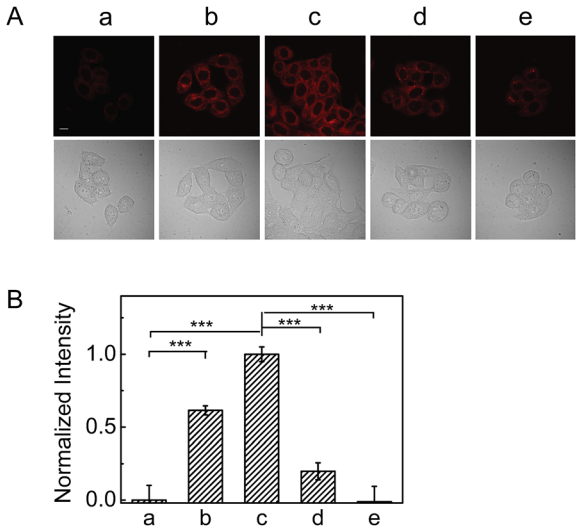

Fig. 2 (A) Confocal fluorescence images of HeLa cells. Cells incubated with NAB (10 μM) for 4 h in the presence of (a) 0, (b) 50, and (c) 100 μM H_2O_2; cells pretreated with H_2O_2 (100 μM) in the presence of (d) 100 μM and (e) 1 mM NAC for 10 min, and then incubated with NAB (10 μM) for 4 h. Scale bar: 10 μm. The second row is the corresponding differential interference contrast (DIC) images. (B) The normalized intensity of the corresponding images in panel A [the pixel intensity is obtained by subtracting that (control) from image a; the fluorescence intensity from image c is defined as 1.0]. The results are the mean ± standard deviation of five cells. ***p < 0.001, two-sided Student's t-test.

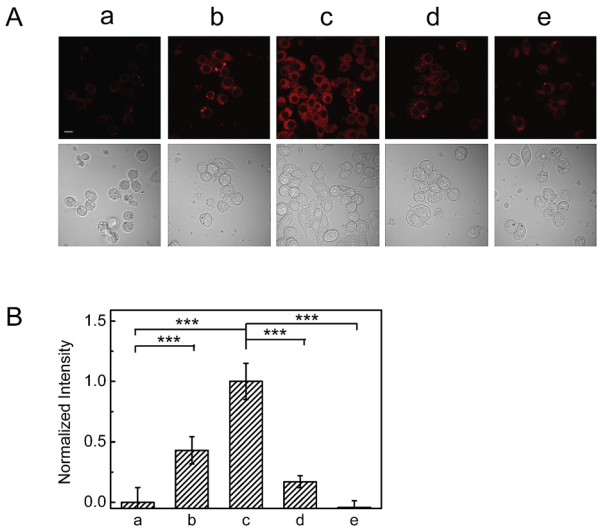

Fig. 3 (A) Confocal fluorescence images of RAW264.7 cells under different conditions. (a) Cells incubated with NAB (10 μM) for 4 h; cells pre-treated with (b) 0.5 and (c) 1 μg mL^{-1} PMA for 1 h and then incubated with NAB (10 μM) for 4 h; cells pre-treated with PMA (1 μg mL^{-1}) in the presence of (d) 100 μM and (e) 1 mM NAC for 1 h and then incubated with NAB (10 μM) for 4 h. Scale bar: 10 μm. (B) Normalized intensity of the fluorescence images in panel A [the pixel intensity is obtained by subtracting that (control) from image a; the fluorescence intensity from image c is defined as 1.0]. The results are presented as mean ± standard deviation of five cells. ***p < 0.001, two-sided Student's t-test.

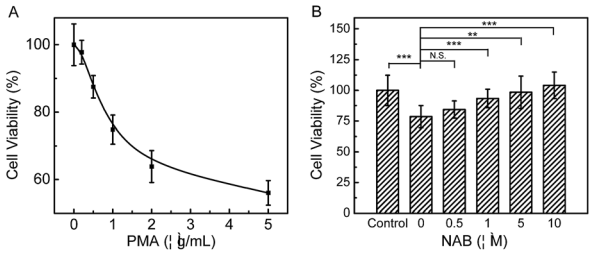

Fig. 4 Cell viability of RAW264.7 cells. (A) Cells treated with PMA at varied concentrations for 1 h; (B) cells treated with PMA (1 μg mL^{-1}) for 1 h and then incubated with NAB at varied concentrations for 4 h. Control is the untreated cells. The results are the mean ± standard deviation of five separate measurements. ***p < 0.001, **p < 0.01, N.S.: no significance, p > 0.01, two-sided Student's t-test.

Protective effect of NAB against cellular inflammation

Since PMA induced inflammation can promote apoptosis through excess oxidative stress in cells, and H_2S has been discovered to alleviate inflammatory response effectively, as a proof of concept, we investigated the protective effect of NAB against inflammation on RAW264.7 cells. As shown in Fig. 4A, after cells are exposed to varied concentrations of PMA for 1 h, the MTT assay manifests that 1 μg mL^{-1} PMA could lead to an about 25% decrease in the cell viability as compared to the control. However, the cells exposed to PMA can significantly recover their viability after they are incubated with NAB, and this viability recovery is increased as the dose of NAB rises. A negative control experiment was also conducted by treating cells with NAH under the same PMA conditions (Fig. S19†), which demonstrates that NAH cannot protect RAW264.7 cells from the stimulation of PMA. Moreover, the ROS scavenging capacity (an anti-inflammatory behavior) of NAB was observed *via* monitoring the intracellular ROS change with a commercial dye CRDR (Fig. S20†). All the above findings disclose that NAB could rescue RAW264.7 cells from PMA induced cellular inflammation possibly *via* scavenging H_2O_2, and might serve as a potential therapeutic H_2S donor.

Conclusions

In summary, we have reported NAB as the first ROS-triggered off-on fluorescent H_2S donor. H_2S release from NAB was detected in both aqueous buffer and live cells. Unlike the previous reported H_2S donors, NAB can achieve H_2S release with a concomitant off-on fluorescence after activated by ROS. More importantly, using NAB, we demonstrated the real-time imaging of H_2S delivery and the cytoprotection against ROS in RAW264.7 cells. The developed fluorescent donor may find a wide use in the delivery and real-time monitoring studies of H_2S in some biosystems.

Conflicts of interest

There are no conflicts to declare.

Acknowledgements

This work is supported by grants from the NSF of China (No. 21820102007, 21675159, 21535009, 91732104, 21775152, 21435007 and 21621062), the Chinese Academy of Sciences (Grant XDB14030102), and Youth Innovation Promotion Association of CAS (2016027).

Notes and references

1 M. W. Zhang, G. Yang, Y. F. Zhou, C. Qian, M. D. Mu, Y. Ke and Z. M. Qian, *J. Cell. Physiol.*, 2019, **234**, 3158–3169.
2 (*a*) L. Li, M. Whiteman, Y. Y. Guan, K. L. Neo, Y. Cheng, S. W. Lee, Y. Zhao, R. Baskar, C. H. Tan and P. K. Moore, *Circulation*, 2008, **117**, 2351–2360; (*b*) M. Kuksis, P. M. Smith and A. V. Ferguson, *PLoS One*, 2014, **9**, e105772.
3 A. P. Lan, X. X. Liao, L. Q. Mo, C. T. Yang, Z. L. Yang, X. Y. Wang, F. Hu, P. X. Chen, J. Q. Feng, D. D. Zheng and L. C. Xiao, *PLoS One*, 2011, **6**, e25921.
4 (*a*) C. Szabo and A. Papapetropoulos, *Pharmacol. Rev.*, 2017, **69**, 497–564; (*b*) Y. Zhao, T. D. Biggs and M. Xian, *Chem. Commun.*, 2014, **50**, 11788–11805.
5 (*a*) J. M. Kang, Z. Li, C. L. Organ, C. M. Park, C. T. Yang, A. Pacheco, D. F. Wang, D. J. Lefer and M. Xian, *J. Am. Chem. Soc.*, 2016, **138**, 6336–6339; (*b*) Y. Zhao, A. K. Steiger and M. D. Pluth, *Angew. Chem., Int. Ed.*, 2018, **57**, 13101–13105.
6 C. R. Powell, J. C. Foster, B. Okyere, M. H. Theus and J. B. Matson, *J. Am. Chem. Soc.*, 2016, **138**, 13477–13480.
7 (*a*) Y. Zhao, A. K. Steiger and M. D. Pluth, *Chem. Commun.*, 2018, **54**, 4951–4954; (*b*) Y. Zhao, H. Wang and M. Xian, *J. Am. Chem. Soc.*, 2011, **133**, 15–17; (*c*) Y. Zhao, M. M. Cerda and M. D. Pluth, *Chem. Sci.*, 2019, **10**, 1873–1878; (*d*) Y. Zhao, S. Bhushan, C. T. Yang, H. Otsuka, J. D. Stein, A. Pacheco, B. Peng, N. O. Devarie-Baez, H. C. Aguilar, D. J. Lefer and M. Xian, *ACS Chem. Biol.*, 2013, **8**, 1283–1290; (*e*) Y. Zhao, C. T. Yang, C. Organ, Z. Li, S. Bhushan, H. Otsuka, A. Pacheco, J. M. Kang, H. C. Aguilar, D. J. Lefer and M. Xian, *J. Med. Chem.*, 2015, **58**, 7501–7511.
8 (*a*) Y. Q. Zheng, B. C. Yu, Z. Li, Z. N. Yuan, C. L. Organ, R. K. Trivedi, S. M. Wang, D. J. Lefer and B. H. Wang, *Angew. Chem., Int. Ed.*, 2017, **56**, 11749–11753; (*b*) A. K. Steiger, M. Marcatti, C. Szabo, B. Szczesny and M. D. Pluth, *ACS Chem. Biol.*, 2017, **12**, 2117–2123.
9 (*a*) N. O. Devarie-Baez, P. E. Bagdon, B. Peng, Y. Zhao, C. M. Park and M. Xian, *Org. Lett.*, 2013, **15**, 2786–2789; (*b*) J. J. Woods, J. Cao, A. R. Lippert and J. J. Wilson, *J. Am. Chem. Soc.*, 2018, **140**, 12383–12387; (*c*) Y. Zhao, S. G. Bolton and M. D. Pluth, *Org. Lett.*, 2017, **19**, 2278–2281.
10 A. K. Steiger, Y. Yang, M. Royzen and M. D. Pluth, *Chem. Commun.*, 2017, **53**, 1378–1380.
11 (*a*) P. Chauhan, S. Jos and H. Chakrapani, *Org. Lett.*, 2018, **20**, 3766–3770; (*b*) Y. Zhao, H. A. Henthorn and M. D. Pluth, *J. Am. Chem. Soc.*, 2017, **139**, 16365–16376; (*c*) Y. Zhao and M. D. Pluth, *Angew. Chem., Int. Ed.*, 2016, **55**, 14638–14642; (*d*) M. D. Hartle and M. D. Pluth, *Chem. Soc. Rev.*, 2016, **45**, 6108–6117.

12 (*a*) Y. C. Chen, C. C. Zhu, J. J. Cen, Y. Bai, W. J. He and Z. J. Guo, *Chem. Sci.*, 2015, **6**, 3187–3194; (*b*) L. W. He, X. L. Yang, K. X. Xu, X. Q. Kong and W. Y. Lin, *Chem. Sci.*, 2017, **8**, 6257–6265; (*c*) S. Xu, H. W. Liu, X. Yin, L. Yuan, S. Y. Huan and X. B. Zhang, *Chem. Sci.*, 2019, **10**, 320–325; (*d*) X. H. Li, X. H. Gao, W. Shi and H. M. Ma, *Chem. Rev.*, 2014, **114**, 590–659; (*e*) Z. Q. Mao, H. Jiang, Z. Li, C. Zhong, W. Zhang and Z. H. Liu, *Chem. Sci.*, 2017, **8**, 4533–4538; (*f*) L. Y. Wu, Y. D. Sun, K. Sugimoto, Z. L. Luo, Y. Ishigaki, K. Y. Pu, T. Suzuki, H. Y. Chen and D. J. Ye, *J. Am. Chem. Soc.*, 2018, **140**, 16340–16352; (*g*) B. Shi, Q. L. Yan, J. Tang, K. Xin, J. C. Zhang, Y. Zhu, G. Xu, R. C. Wang, J. Chen, W. Gao, T. L. Zhu, J. Y. Shi, C. H. Fan, C. C. Zhao and H. Tian, *Nano Lett.*, 2018, **18**, 6411–6416.

13 D. J. R. Stone and S. Yang, *Antioxid. Redox Signaling*, 2006, **8**, 243–270.

14 L. C. Lo and C. Y. Chu, *Chem. Commun.*, 2003, 2728–2729.

15 (*a*) R. H. Burdon, *Free Radical Biol. Med.*, 1995, **18**, 775–794; (*b*) M. Abo, Y. Urano, K. Hanaoka, T. Terai, T. Komatsu and T. Nagano, *J. Am. Chem. Soc.*, 2011, **133**, 10629–10637.

16 (*a*) M. C. Y. Chang, A. Pralle, E. Y. Isacoff and C. J. Chang, *J. Am. Chem. Soc.*, 2011, **133**, 15–17; (*b*) M. Giorgio, M. Trinei, E. Migliaccio and P. G. Pelicci, *Nat. Rev. Mol. Cell Biol.*, 2007, **8**, 722–728; (*c*) J. Liu, J. Ren, X. J. Bao, W. Gao, C. L. Wu and Y. B. Zhao, *Anal. Chem.*, 2016, **88**, 5865–5870.

17 C. R. Liu, J. Pan, S. Li, Y. Zhao, L. Y. Wu, C. E. Berkman, A. R. Whorton and M. Xian, *Angew. Chem., Int. Ed.*, 2011, **50**, 10327–10329.

18 J. Xu, Y. Zhang, H. Yu, X. D. Gao and S. J. Shao, *Anal. Chem.*, 2016, **88**, 1455–1461.